QUIET: **Q**uantifying **U**nderutilized **I**nfluential **E**dges for **T**argeted Synchronization

Sovesh Mohapatra[1], Christoffer G. Alexandersen[1], Panos Fotiadis[2], Dani S. Bassett[1-3-6]

[1]Department of Bioengineering, University of Pennsylvania, Philadelphia, PA 19104; [2]Department of Anesthesiology, University of Michigan, Ann Arbor, MI 48109; [3]Department of Psychiatry, [4]Department of Physics & Astronomy, [5]Department of Neurology, [6]Department of Electrical & Systems Engineering, University of Pennsylvania, Philadelphia, PA 19104

Introduction

Human brains navigate a complex energy landscape, steering neural activity through a relatively fixed structural connectome to support diverse cognitive functions. Network control theory (NCT) formalizes this process by quantifying the energetic cost of transitions between brain states. Standard NCT operates at the level of nodes, implicitly assuming that every structural connection transmits a control signal at full capacity regardless of the endogenous activity it already carries. This assumption obscures a critical question: which specific white-matter pathways should carry a control signal, and which should remain quiescent. Here, we introduce Quantifying Underutilized Influential Edges for Targeted Synchronization (QUIET), an edge-centric framework that integrates structural controllability with information-theoretic measures of functional coupling. QUIET ranks each white-matter connection by its structural leverage relative to its functional redundancy, identifying quiet highways: edges that are structurally influential yet functionally underutilized and therefore most amenable to energy-efficient perturbation across synthetic networks, healthy adults, and pharmacologically sedated brains. This edge-level reframing opens a route to pathway-selective, low-energy steering of brain network dynamics.

Methodology Overview

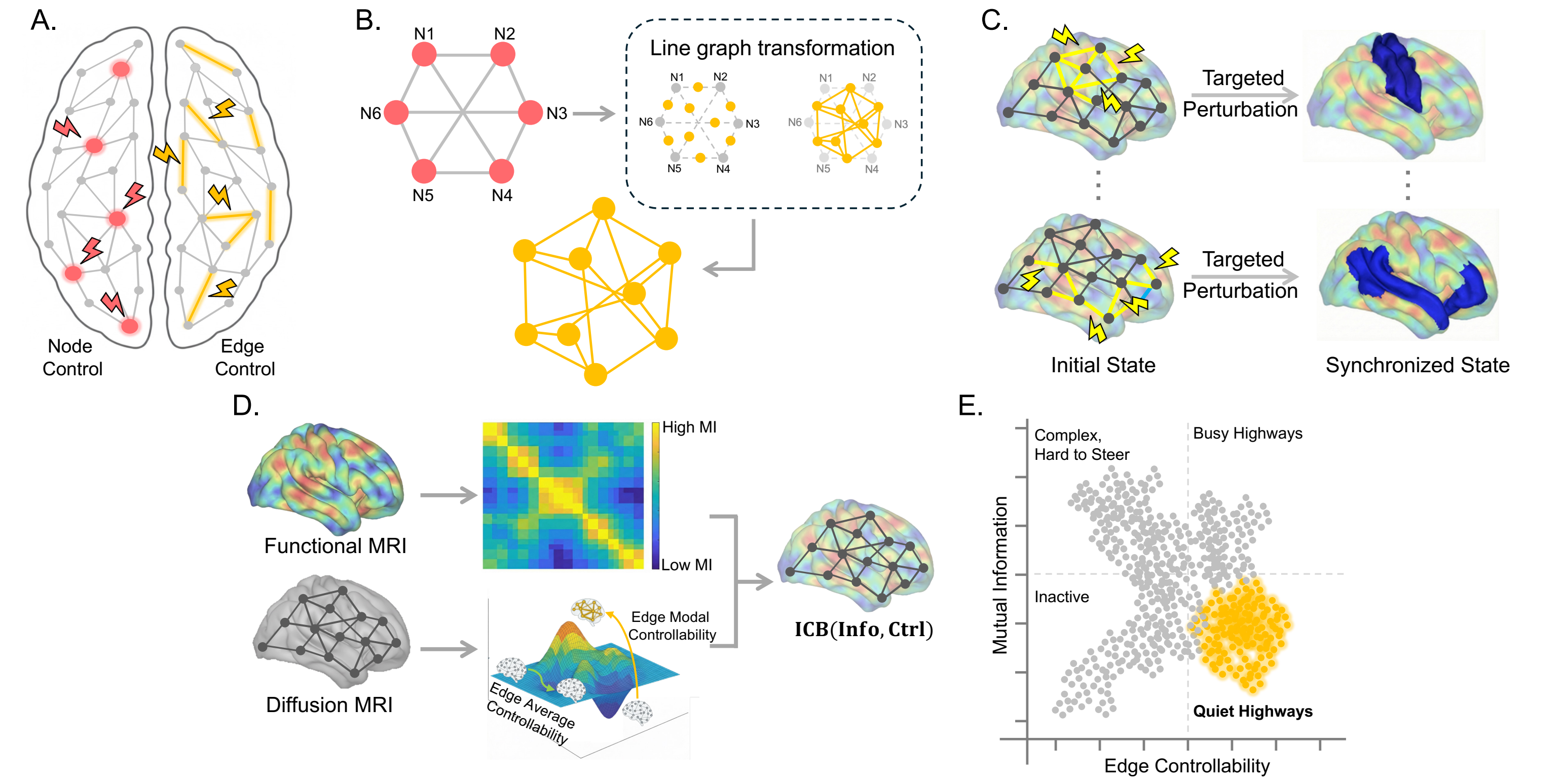

Fig 1. QUIET reframes network control as an edge-level problem. (A) Node-centric control perturbs regions whereas edge-centric targets tracts. (B) The line graph yields edge-level controllability. (C) Selected edges (yellow) synchronize the target region (blue). (D) fMRI provides mutual information (MI). dMRI provides controllability (eAC, eMC). (E) Quiet highways (mustard): high controllability, low MI.

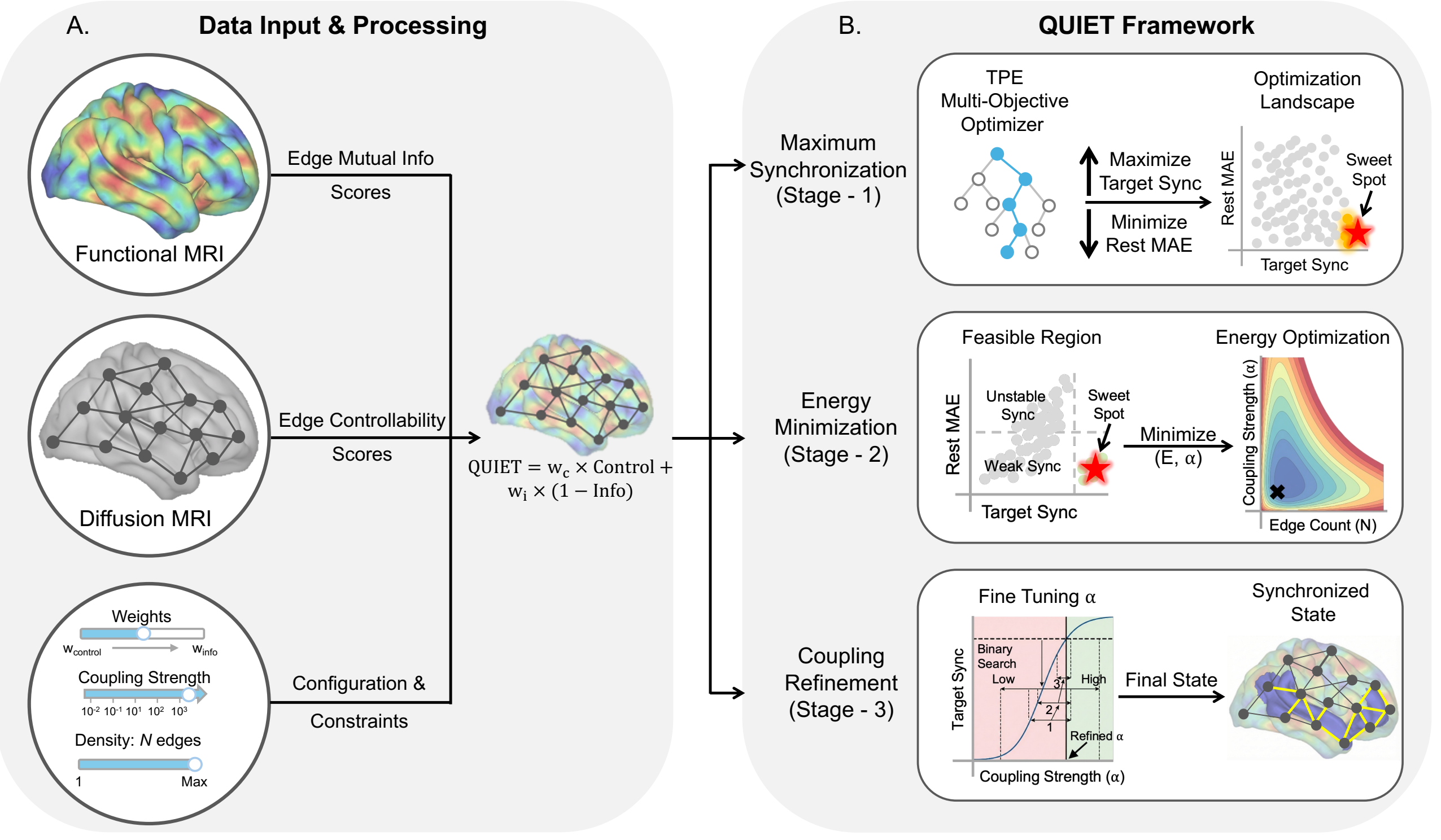

Fig 2. QUIET's three-stage optimization pipeline. (A) fMRI-derived MI and dMRI-derived controllability combine into the QUIET score. (B) Stage 1 maximizes target synchronization, Stage 2 minimizes energy, Stage 3 refines coupling α.

Results

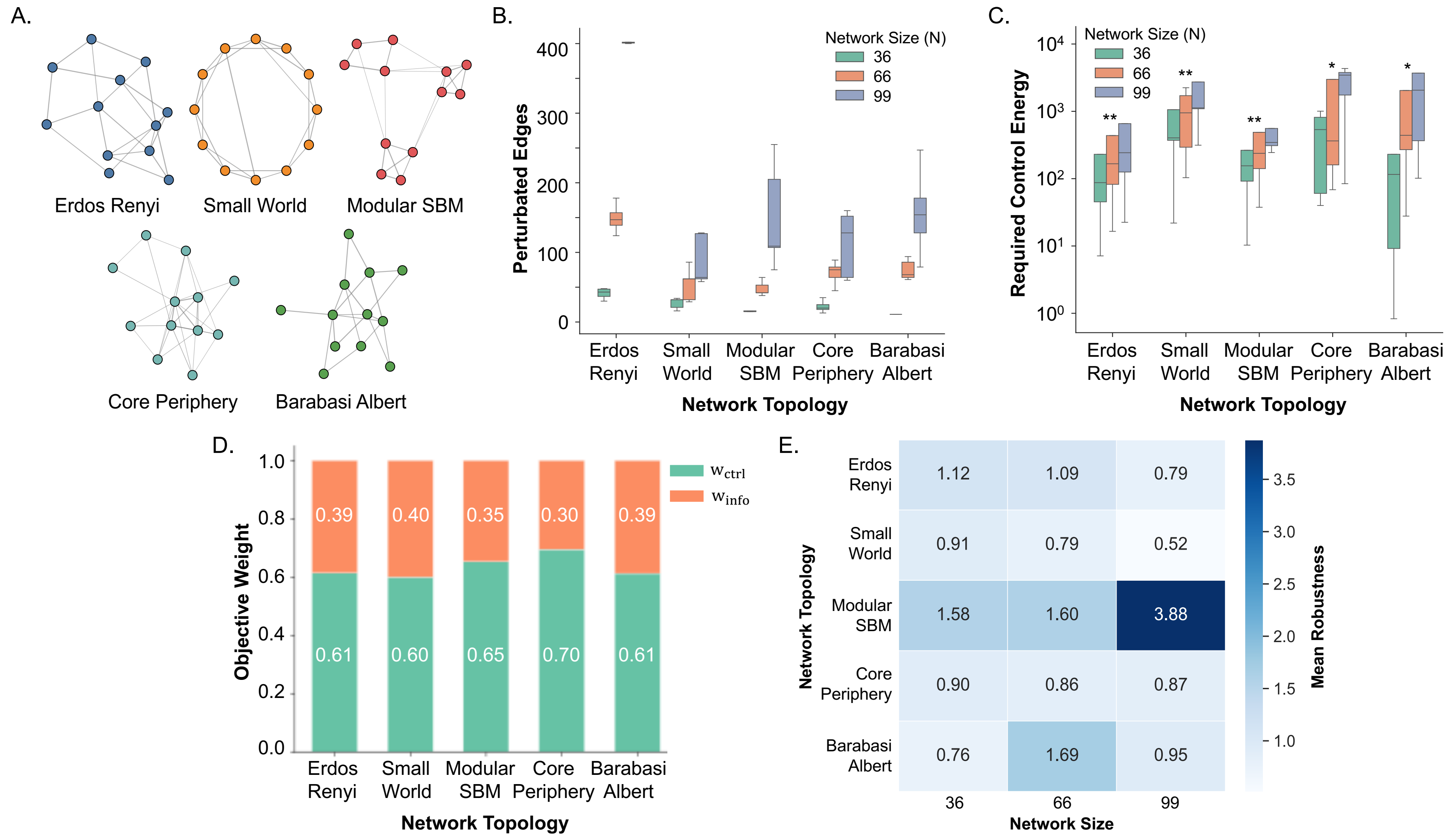

	36	66	99
Erdos Renyi	1.12	1.09	0.79
Small World	0.91	0.79	0.52
Modular SBM	1.58	1.60	3.88
Core Periphery	0.90	0.86	0.87
Barabasi Albert	0.76	1.69	0.95

Fig 3. QUIET generalizes across topologies, scales, and coupling regimes. (A) Five synthetic topologies tested at three sizes (N = 36, 66, 99) and five coupling strengths. (B) Perturbed edge count per topology and scale. (C) Control energy across topologies and scales. (D) Optimized ranking weights w_ctrl (green) and w_info (orange), averaged across coupling strengths. (E) Mean robustness across topology–size combinations.

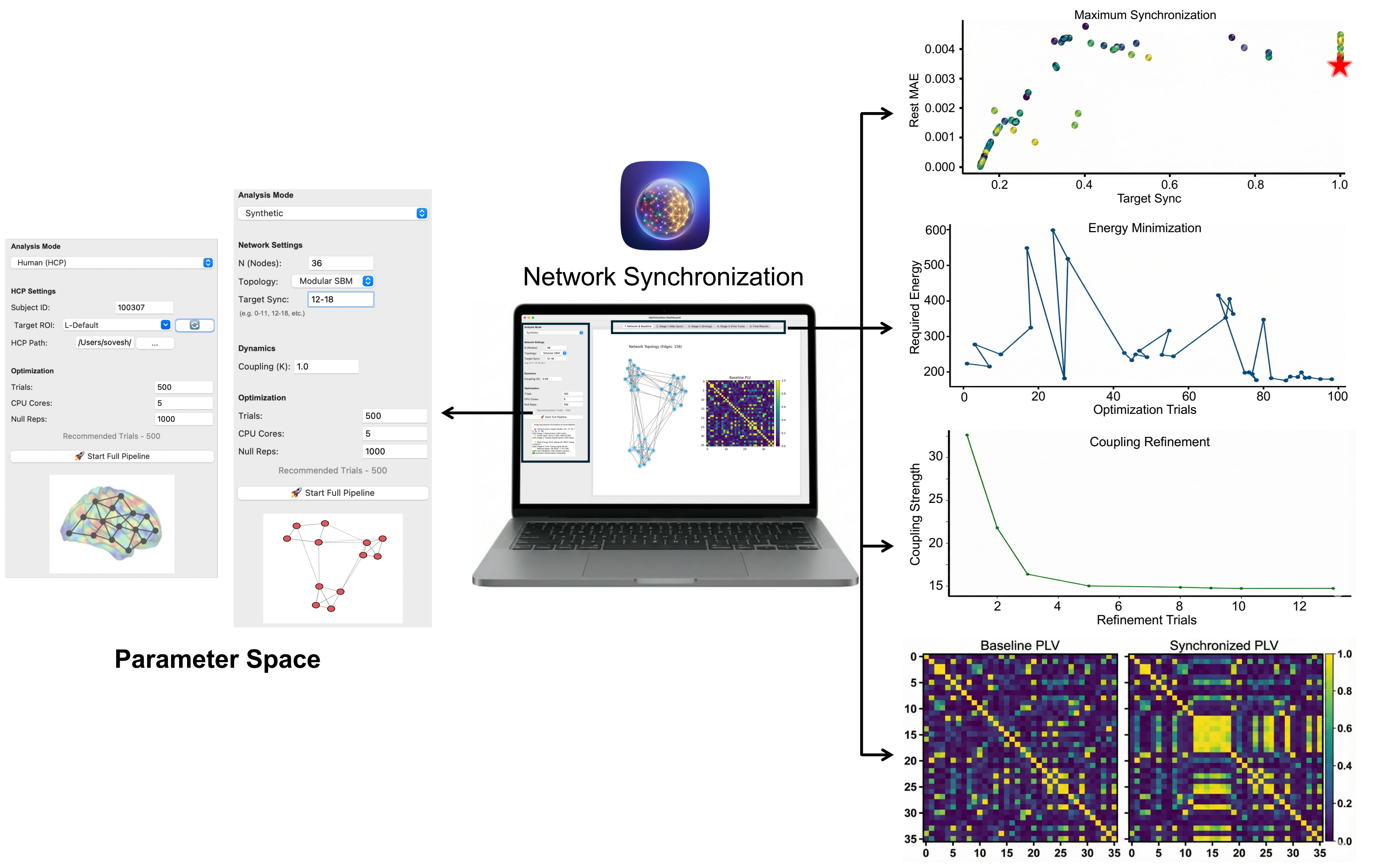

Fig 4. Network Synchronization: open-source software for edge-centric control. Two modes (synthetic, empirical) configure inputs (left) and run the full QUIET pipeline. Outputs (right) include the Pareto front with sweet spot, energy convergence, coupling α refinement, and baseline vs. synchronized PLV matrices.

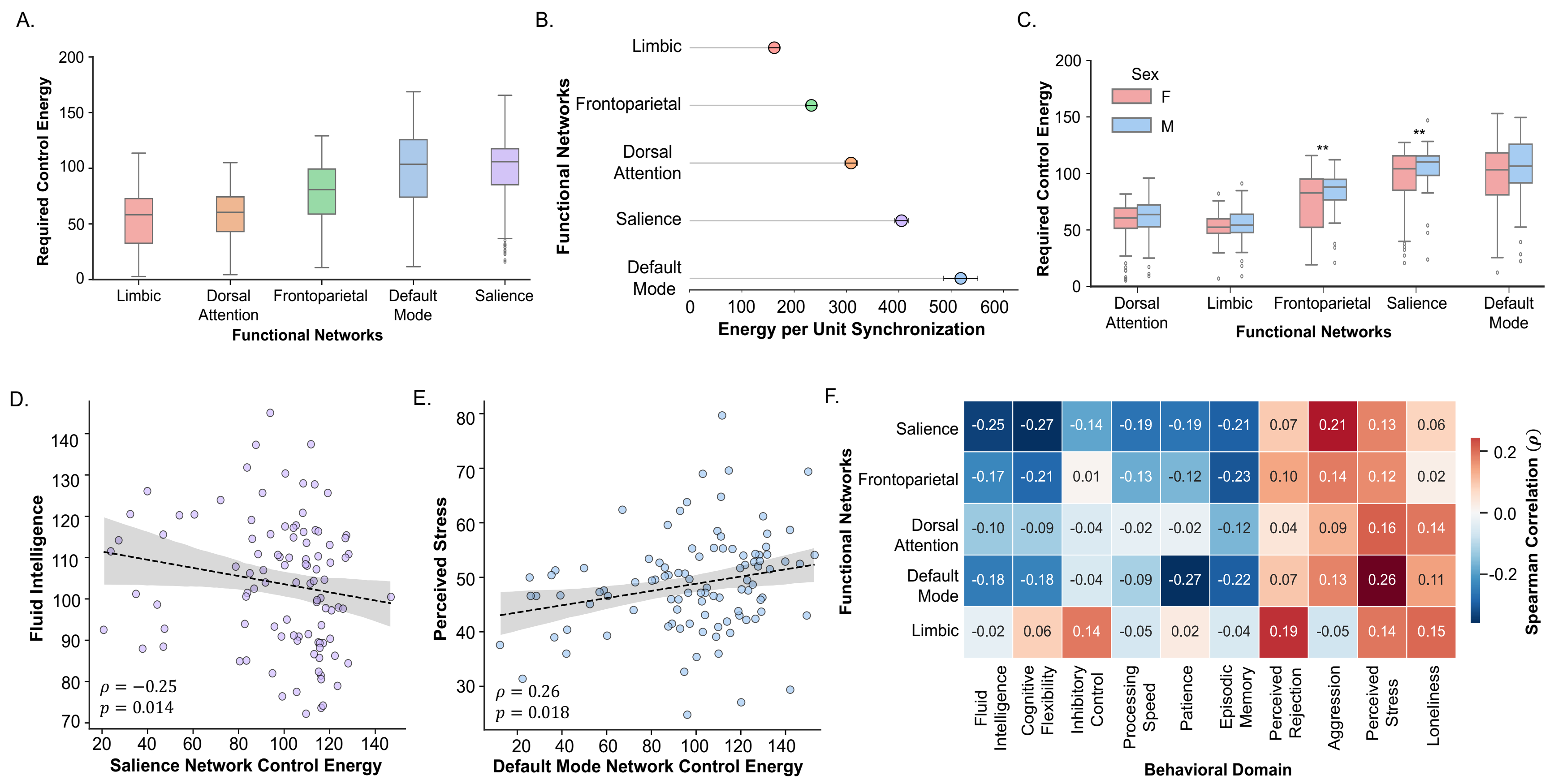

	Fluid Intelligence	Cognitive Flexibility	Inhibitory Control	Processing Speed	Patience	Episodic Memory	Perceived Rejection	Aggression	Perceived Stress	Loneliness
Salience	-0.25	-0.27	-0.14	-0.19	-0.19	-0.21	0.07	0.21	0.13	0.06
Frontoparietal	-0.17	-0.21	0.01	-0.13	-0.12	-0.23	0.10	0.14	0.12	0.02
Dorsal Attention	-0.10	-0.09	-0.04	-0.02	-0.02	-0.12	0.04	0.09	0.16	0.14
Default Mode	-0.18	-0.18	-0.04	-0.09	-0.27	-0.22	0.07	0.13	0.26	0.11
Limbic	-0.02	0.06	0.14	-0.05	0.02	-0.04	0.19	-0.05	0.14	0.15

Fig 5. Control energy to synchronize functional networks (HCP, n = 100). (A) Energy per network. (B) Energy per synchronization gain. (C) Females require less than males for frontoparietal and salience (**, $p < 0.05$). (D) Salience energy vs. fluid intelligence. (E) Default-mode energy vs. perceived stress. (F) Full energy–behavior landscape.

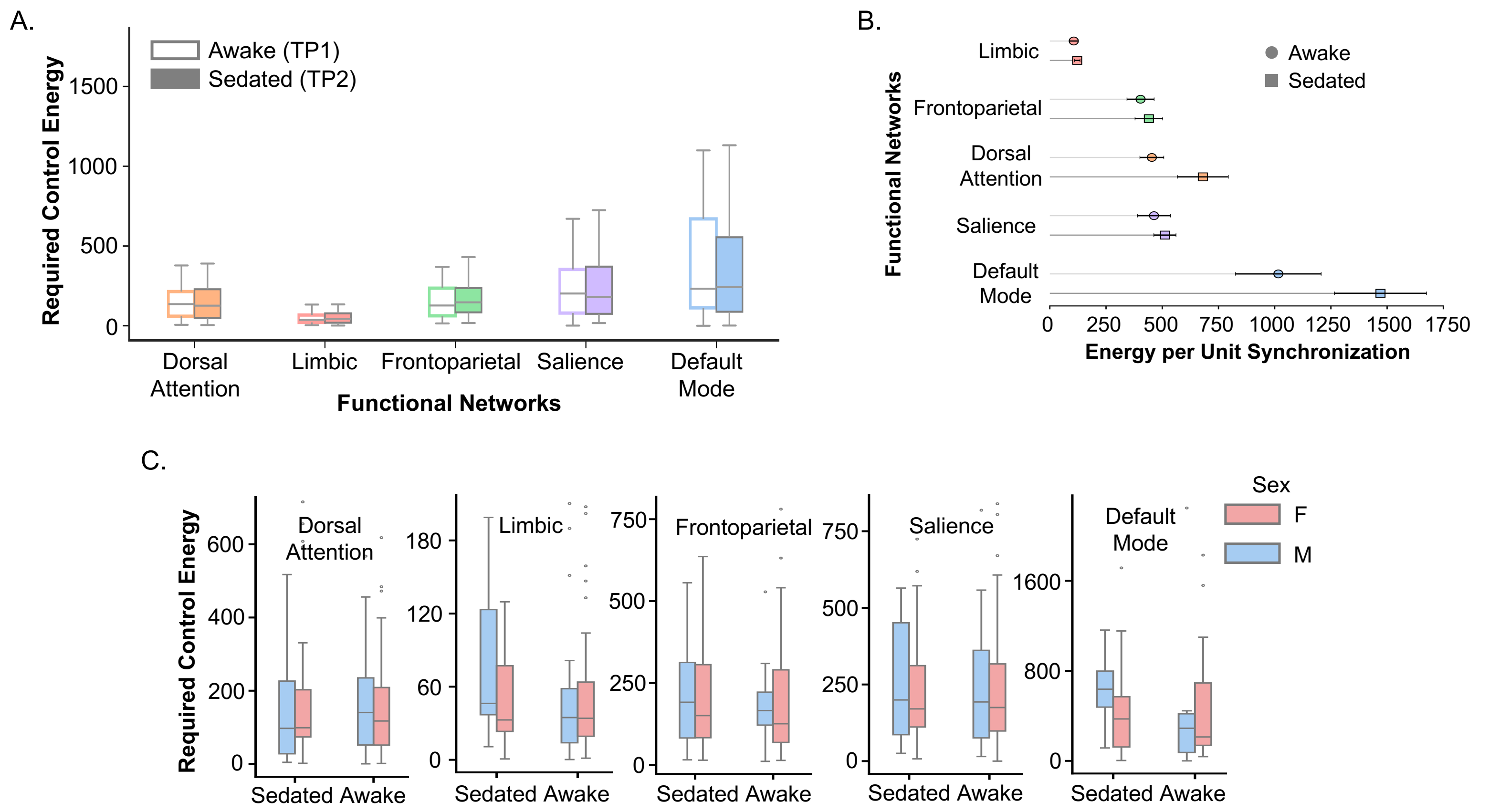

Fig 6. Sedation increases the energetic cost of network synchronization. (A) Energy across five networks: awake (TP1, open) and sedated (TP2, filled). (B) Energy per synchronization gain, awake (circle) vs. sedated (square). (C) Sex-stratified energy. Females < males for limbic under sedation (**, $p < 0.05$).

Conclusions

QUIET shifts network control from nodes to edges, identifying quiet highways, structurally influential yet functionally underutilized connections, by ranking each white-matter pathway by its structural leverage relative to its functional redundancy. The framework generalizes across synthetic topologies, healthy participants from the Human Connectome Project, and an independent anesthesia cohort. Salience-network control energy tracks fluid intelligence and cognitive flexibility, while default-mode energy tracks perceived stress. Dexmedetomidine sedation raises the energetic cost of synchronizing higher-order networks. Released as open-source software, QUIET predicts energy-efficient synchronization pathways and generates testable predictions for stimulation experiments aimed at individualized circuit-level intervention.

Complex Systems